Send Orders for Reprints to reprints@benthamscience.ae

RESEARCH ARTICLE

Silver Nanoparticles with High Loading Capacity of Amphotericin B: Characterization, Bactericidal and Antifungal Effects

Victoria Leonhard[1,2], Roxana V. Alasino[1,2], Adrián Muñoz[2] and Dante M. Beltramo[1,2,3,*]

[1]*Consejo Nacional de Investigaciones Científicas y Técnicas, Conicet - Argentina;* [2]*Centro de Excelencia en Productos y Procesos de Córdoba, Ceprocor - Argentina;* [3]*Laboratorio de Biotecnología - Facultad de Ciencias Químicas - Universidad Católica de Córdoba - Argentina*

ARTICLE HISTORY

Received: March 31, 2017
Revised: July 11, 2017
Accepted: September 06, 2017

DOI:
10.2174/1567201814666170918162337

Abstract: The purpose of this study was to evaluate the most appropriate conditions to generate silver nanoparticles (AgNPs) loaded with a potent antimycotic drug like amphotericin B (AmB), characterize the physicochemical properties, and to evaluate the cytotoxic effect and biological activity of these new nanostructures as a potential nanocarrier for hydrophobic drugs. It was determined that the optimal molar ratio between Ag and AmB is 1/1 given the uniformity of size around 170 nm of the nanoparticles generated as well as their strongly negative ζ potential of -35 mV, a condition that favors repulsions between AgNPs and inhibiting their aggregation. In this condition, only 0.8 $mg.mL^{-1}$ of Ag is needed to solubilize 5 $mg.mL^{-1}$ of AmB, a concentration currently used in commercial formulations. It is important to emphasize that the loading capacity (w/w) of this nanostructure is much higher than that of micellar and liposomal formulations.

These AgNP-AmB nanoparticles retain both the bactericidal effect of silver and the cytotoxic and antifungal effect of AmB. However, it was shown that these nanoparticles are spontaneously associated with plasma lipoproteins (LDL and HDL), inhibiting their cytotoxic effects on red blood cells and on at least two cell lines, Vero and H1299 and slightly reducing its bactericidal effect on P. aeruginosa. In contrast, the antifungal effect of the formulation is maintained and is even higher than that when the nanoparticle is not associated with lipoproteins, indicating that this association is of the reversible type.

The characterization of these nanoparticles is discussed as a potential new model formulation able to improve the antifungal therapeutic efficiency of AmB.

Keywords: Silver Nanoparticles, Amphotericin B, bactericidal effect, antifungal effect, plasma lipoproteins.

1. INTRODUCTION

Currently, nanobiotechnology plays an essential role in the therapy of cancer and various diseases because it improves the efficiency of drug administration, reduces adverse side effects of the drug and increases molecular targeting in biomedical applications. Nanomaterials are also considered as promising solutions to problems of stability and aqueous solubility, achieving intelligent and controllable morphologies whose surface can be functionalized. Among them, metallic nanoparticles (NPs) are one of the most commercially available nanomaterials [1].

Metallic NPs are of particular technological interest due to their multiple and diverse optical, catalytic, magnetic, electronic and, in some cases, also bactericidal properties [2-5]. These can be defined as isolated aggregates smaller than 100 nm, generally formed by the clustering of metal atoms such as silver, gold, platinum, palladium, which are sometimes surrounded by a stabilizing capsule that prevents them from agglomerating [6-8].

There are several methods to prepare metallic NPs such as chemical reduction of a metal salt, electrochemical synthesis, ligand reduction and ligand displacement in organometallic compounds, thermal decomposition, photochemistry or thermochemistry, among others [9-11]. One of the methods most widely used is the chemical reduction of transition metal salts in the presence of stabilizing agents, since it has the advantage of being highly reproducible, giving rise to monodisperse colloids with narrow particle size distribution [12, 13].

Silver NPs (AgNPs) exist in a wide variety of sizes (from few to hundreds of nm) and shapes (spheres, wires, rods, etc.), and are further differentiated by their coating (Citrate, peptides, polymers, sugars, etc.). These have drawn wide

*Address correspondence to this author at the Centro de Excelencia en Productos y Procesos de Córdoba, Ceprocor, Ministerio de Ciencia y Tecnología de Córdoba, Pabellón Ceprocor, CP 5164, Santa María de Punilla, Córdoba - Argentina; Tel: 54-3541-489651/53 ext.143;
Fax: 54-3541-488181; E-mails: dantemiguelbeltramo@gmail.com; dbeltramo@ceprocor.uncor.edu

1567-2018/17 $58.00+.00 **© 2017 Bentham Science Publishers**

attention because of their potent antimicrobial, antifungal, antiangiogenic and anti-inflammatory activity [14, 15].

Naked AgNPs are quite unstable in suspension [16], thus different types of coatings are currently used to decrease the agglomeration [17] and dissolution of the NPs [18] as well as to modify their biological activity [17-19].

The stability of AgNPs strongly influences their toxicity, since silver ions are considered one of the main toxicity factors of silver [18]. It was reported that agglomeration of the NPs also potentiates its toxicity [20].

Polymeric water-soluble materials such as polyvinylpyrrolidone (PVP), polyethyleneglycol (PEG), polyethyleneimine (PEI), oligosaccharides, polysaccharides, and polyelectrolytes, are usually used to avoid agglomeration and precipitation of the NPs [21]. In general, it is understood that the magnitude of the biological effect produced by AgNPs depends on their size, shape, agglomeration and the nature of the functionalizing agents [22].

On the other hand, amphotericin B (AmB) is a potent antifungal that is still widely used in the treatment of systemic fungal infections despite having high toxicity and requiring parenteral administration due to malabsorption from the gastrointestinal tract [23, 24]. Its structure (Fig. **1**), which comprises a hydrophobic heptane chain and a hydroxyl-rich hydrophilic chain, imparts an amphoteric character to the molecule which results in insignificant solubility in aqueous medium. This poor aqueous solubility has led to the development of multiple formulations of AmB to reduce the complications associated with its parenteral administration, including renal toxicity [25, 26].

In this work we describe the interaction of bactericide AgNPs and antifungal AmB, with the aim of characterizing the physicochemical properties of AgNP-AmB complex, the loading capacity of AmB, and the biological effect and *in vitro* toxicity after the specific interaction with plasma lipoproteins (LDL and HDL). The association with lipoproteins caused a slight reduction in the bactericidal capacity of the AgNP and a large reduction in the cytotoxicity produced by AmB; however, the antifungal capacity was higher than that of the lipoprotein-free formulation.

2. MATERIALS AND METHODS

2.1. Materials

Silver nitrate ($AgNO_3$) and sodium tetraborohydride ($NaBH_4$) were purchased from Sigma Aldrich, Argentina. Polyethyleneglycol 4000 (PEG) was purchased from Parafarm, Argentina. Amphotericin B (AmB) was a gift from NANOX Release S.A., Argentina. Amfostat (AFS) and Anfogen (AFG) were purchased from Bristol Myers Squibb Argentina S.R.L. and from Genpharma S.A. Argentina, respectively. All cell reagents used were from Invitrogen, Argentina. All other chemicals and solvents used were of analytical grade.

2.2. Methods

2.2.1. Synthesis of AgNPs

The synthesis of AgNPs was carried out by chemical reduction of $AgNO_3$ using $NaBH_4$ as a reducing agent. The optimized synthesis procedure involved dropwise addition of an aqueous solution of $AgNO_3$ (0.001 M, 2 mL) to an aqueous solution of $NaBH_4$ (0.002 M, 30 mL) maintained previously with stirring in ice bath for 20 minutes. A change in the color of the solution from colorless to yellow indicated the formation of NPs. After the addition of $AgNO_3$, the stirring was stopped. This stock solution of AgNPs was maintained at 4 °C and in darkness, remaining stable for up to one month under these conditions. UV-visible spectroscopy was used to evidence the formation of NPs.

2.2.2. Preparation of AgNP-AmB

AmB stock solution was prepared by dissolving the solid drug in dimethylsulfoxide (DMSO) at a concentration of 30 $mg.mL^{-1}$. This solution was prepared in the dark using nitrogen to protect the drug from oxidation.

The loading of AmB into AgNPs was performed by slowly adding increasing amounts of the drug to the AgNPs solution at 4 °C reaching different Ag/AmB molar ratios: 1/1; 1/5; 1/10; 1/15; 1/30; 1/60; 1/120. After stirring for 5 minutes, the samples were incubated for 24 hours at 4 °C in the dark. Subsequently, the centrifugation of the mixtures was performed at 15,000 *xg* for 10 minutes to remove the unbound AmB; the supernatant was dialysed against bidis-

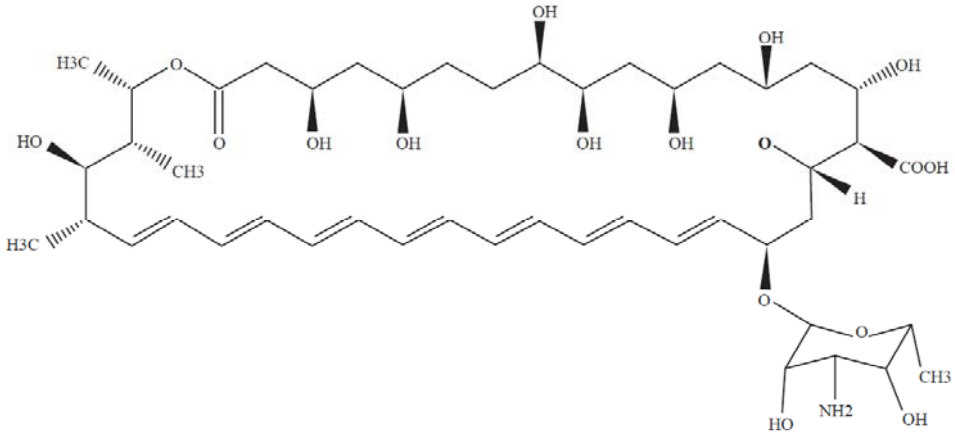

Fig. (1). Chemical structure of AmB.

tilled water for 24 hours at 4 °C in the dark using SpectraPor dialysis membranes with a molecular weight cut of 14,000 Da to remove DMSO and any unbound material.

2.2.3. Determination of AmB Concentration

Quantification of AmB is performed spectrophotometrically by its absorption at 405 nm after dilution in methanol to achieve complete monomerization of the drug and to become independent of its state of aggregation as described by Gaboriau *et al* [27].

Spectroscopic determinations were performed on a Perkin Elmer lambda 25 spectrophotometer.

The drug concentration in each sample was obtained using a calibration curve from 1 $\mu g.mL^{-1}$ to 10 $\mu g.mL^{-1}$ of AmB in 50 % v/v methanol.

2.2.4. Physical and Chemical Characterization of AgNP-AmB

2.2.4.1. Determination of Size and ζ Potential by DLS

The size distribution and ζ potential of NPs were determined using dynamic light scattering (DLS) Malvern Instrument NANO ZS at a fixed scattering angle of 173°.

2.2.4.2. Lyophilization and Resuspension

AgNP-AmB were frozen at -80 °C for 24 hours and then subjected to the lyophilization process. They were then resuspended with a solution of PEG 4000 at 4 % w/v in a volume enough to reach concentrations of AmB of 5 $mg.mL^{-1}$. This concentration was measured as previously mentioned.

2.2.5. In-vitro Studies

2.2.5.1. Hemolysis

Blood was extracted from healthy human volunteers; EDTA was used as an anticoagulant. This sample was washed twice with 9 volumes of saline with 0.9 % NaCl. After each wash, blood cells were pelleted by centrifugation at 1,500 *xg* for 10 minutes and the supernatant was discarded. Finally, the sample was adjusted to 4 x 10^7 $cells.mL^{-1}$.

The hemolytic activity of AgNPs and different AgNP-AmB complexes (with an AmB concentration of 0.1 $mg.mL^{-1}$) was studied by adding 1 volume of the red blood cell suspension to 1 volume of solution with AgNPs. This solution contains: A) Bare AgNPs diluted in half with 0.9 % NaClsolution; B) AgNP-AmB:1/1 diluted in half with 0.9 % NaCl solution; C) AgNP-AmB:1/1 previously incubated for 2 hours at 37 °C with 1 volume of human plasma; D) AgNP-AmB:1/1 previously incubated for 2 hours at 37 °C with 1 volume of purified albumin at 45 $mg.mL^{-1}$; E) AgNP-AmB:1/1 previously incubated for 2 hours at 37 °C with 1 volume of purified LDL or HDL at a cholesterol concentration of 1 $mg.mL^{-1}$. 100 % hemolysis control was obtained by incubating 1 volume of the red blood cells with 1 volume of bi-distilled water.

Samples were incubated for 1 hour at 37 °C and then centrifuged at 15,000 *xg* for 10 minutes. The supernatants were read spectrophotometrically at 540 nm to evidence the presence of free hemoglobin, indicative of cell lysis. Hemolysis percentages of the different samples were calculated based on the comparison of their absorbance value with the 100 % hemolysis control.

2.2.5.2. Cytotoxic Effect on Cell Cultures

Vero (African green monkey kidney epithelial) and H1299 (human non-small cell lung carcinoma) cell lines were maintained in minimal essential medium (MEM) and in DMEM-F12 medium, respectively supplemented with 10 % heat-inactivated fetal bovine serum (FBS-NATOCOR, Córdoba, Argentina), 2 mM L-glutamine and 10 $\mu g.mL^{-1}$ gentamicin at 37 °C and at 5 % CO_2. All cell reagents used were from Invitrogen.

To perform the experiments, the cells were seeded in 96 well plates and after 24 hours of incubation, 100 µL of serial dilutions of AmB from 5 to 20 $\mu g.mL^{-1}$ present in AgNP-AmB:1/1, AgNP-AmB:1/1+plasma, Amfostat (AmB in deoxycholate micelles) and Anfogen (liposomal AmB) were added and incubated for another 24 hours at 37 °C. Bare AgNP was used as control.

Photographs were taken prior to assessing cytotoxicity by the MTT assay. Briefly, in this assay 50 µL of the MTT reagent was added to each well and then cells were incubated for 4 hours at 37 °C. The medium was then discarded and 100 µL of DMSO was added in each well. Soluble formazan was measured at 595 nm using a microplate spectrophotometer (Anthos reader 2010). The percent of cell viability of each sample tested was obtained by comparing its absorbance obtained after the MTT assay with respect to the absorbance obtained by the control of normal cell growth.

Each assay was performed in triplicate.

2.2.5.3. Antimicrobial Activity of AgNPs and AgNP-AmB Against Pseudomonas aeruginosa

The antimicrobial effects of the formulations of AgNPs against P. aeruginosa, as a model of gram negative bacteria, were studied.

An aliquot of 100 µL of AgNPs, AgNP-AmB:1/1, AgNP-AmB:1/1+plasma solutions, with a silver concentration of 60 $\mu g.mL^{-1}$, were incubated with 50 µL of an inoculum of P. aeruginosa (~ $10^7 CFU.mL^{-1}$) in sterile 1.5 mL tubes. The tubes were mixed and incubated for 4 hours in a culture oven with air atmosphere at 35 ± 2 °C. 100 µL of the tested material were then taken and separately placed in sterile Petri dishes with the immediate addition of 20 mL of BHI agar medium (preserved in a 45 °C bath) supplemented with 5 µL of a 1 % w/v TTC (2,3,5-triphenyl-2H-tetrazolium chloride).

Each plate was mixed to homogenize and then allowed to solidify at room temperature. The solidified plates were incubated inverted for a period of 24 hours in a culture oven with air atmosphere at 35 ± 2 °C. In addition, plaques were added with the respective sterility controls of culture media and inputs, plus a positive control by directly seeding the Pseudomonas aeruginosa ATCC No. 23522 (KWIK-STIK Microbiologics) inoculum.

2.2.5.4. Antifungal Activity on Candida albicans

The minimum inhibitory concentrations (MIC) of AmB on C. albicans were determined by a modified version of the

M27-Amethod [28]. Briefly, 100 µL of the yeast inoculum at a concentration of 0.5 x 10^3 to 2.5 x 10^3 CFU.mL^{-1} were added in each well containing serial dilutions of AmB (as AgNP-AmB:1/1, AgNP-AmB:1/1+plasma, Anfogen and Amfostat formulations). Controls of fungus growth alone and in the presence of naked AgNPs were performed.

After 24 hours of incubation at 37 °C, the optical density at 620 nm of each well was read using a microplate spectrophotometer (Anthos Reader 2010).

MIC values are defined as the lowest concentration that prevents visible fungal growth, compared to control growth.

3. RESULTS

3.1. Characterization of Physical Properties of AgNPs

The synthesis of AgNPs was carried out by chemical reduction of $AgNO_3$ using $NaBH_4$ as reducing agent. The techniques of UV-Vis spectroscopy and dynamic light scattering (DLS) confirmed the formation of AgNPs. It is observed in Fig. (**2a**) that the AgNPs prepared have a maximum absorption peak at 395 nm. The presence of this single peak strongly evidences that no NPs aggregation occurred.

The hydrodynamic size and surface charge of the AgNPs were measured using DLS. Both measurements are good indicators of AgNP aggregation status. Under these experimental conditions, the coexistence of two populations of AgNPs was observed, a majority population (70 %) with a hydrodynamic radius of 49,52±27.95 nm and another population of smaller NPs (30 %) of 4,71±2,44 nm (Fig. **2b**).

In addition, an average ζ potential of -27 mV was measured (data not shown). The negative charge stabilizes AgNPs by creating electrostatic repulsions between particles, preventing aggregation.

3.2. Solubilization of AmB in AgNPs

Here we evaluate the ability of these nanostructures to solubilize a hydrophobic drug like AmB. Fig. (**3a**) shows that 5.5 µg.mL^{-1} of Ag can solubilize a maximum amount of AmB of about 1.5 mg.mL^{-1} (1500 µg.mL^{-1}) in Ag/AmB:1/60 molar ratio. This implies that under these conditions, AgNPs can solubilize up to 270 times their own AmB concentration. However, under these loading conditions the structures that are formed have a very large size (1100 nm) and a zeta potential closer to zero (-18 mV), two conditions that are unfavorable and undesired (Fig. **3b** and **3c**).

It is observed that up to the 1/10 molar ratio, the complexes have a size smaller than 150 nm and more negative ζ potentials (greater than -24 mV). With the addition of more AmB the structures increased drastically its size and decreased its ζ potential, indicating that they are much more unstable (Fig. **3b** and **3c**). The minority population of AgNPs of 5 nm was only observed in the Ag/AmB:1/1 molar ratio. By adding more AmB, this second population of NPs disappears (data not shown).

Regarding the aggregation state of AmB, it was found that, in most conditions, AmB appears in an aggregate state, with the characteristic absorption peak at 333 nm (Fig. **3d**). In the 1/1 molar ratio, where less AmB is bound to AgNPs, there is 30 % more AmB in monomeric form than in the other molar ratios. This change in aggregation state is probably due to the fact that once the NP is saturated with AmB on its surface, the addition of larger amounts of AmB causes it to self-aggregate in order to remain soluble in aqueous solution. Thus, self-aggregated drug layers would be formed surrounding the AgNP and probably due to this, the structure shows high loading capacity.

In the 1/120 molar ratio, it was observed that the drug also adopts a mostly monomeric aggregation state. This evidently has to do with a break point in the AmB loading by the NPs where the extreme drug aggregate causes a destabilization or rearrangement of the structure, reducing its loading capacity and forming structures of micrometric size.

Based on these results it was decided to continue the work with smaller Ag/AmB molar ratios: 1/1, 1/5 and 1/10.

3.3. Stability of AgNP-AmB after Lyophilization and Resuspension

The lyophilization process of different AgNP-AmB complexes was carried out to concentrate the samples and perform the *in vitro* assays. These samples were resuspended with a solution of PEG 4000 at 4 % (w/v). This is a molecule that has already been shown to be particularly effective in coating AgNPs and improving their stability [29, 30], probably due to the fact that it is a very flexible and water-soluble

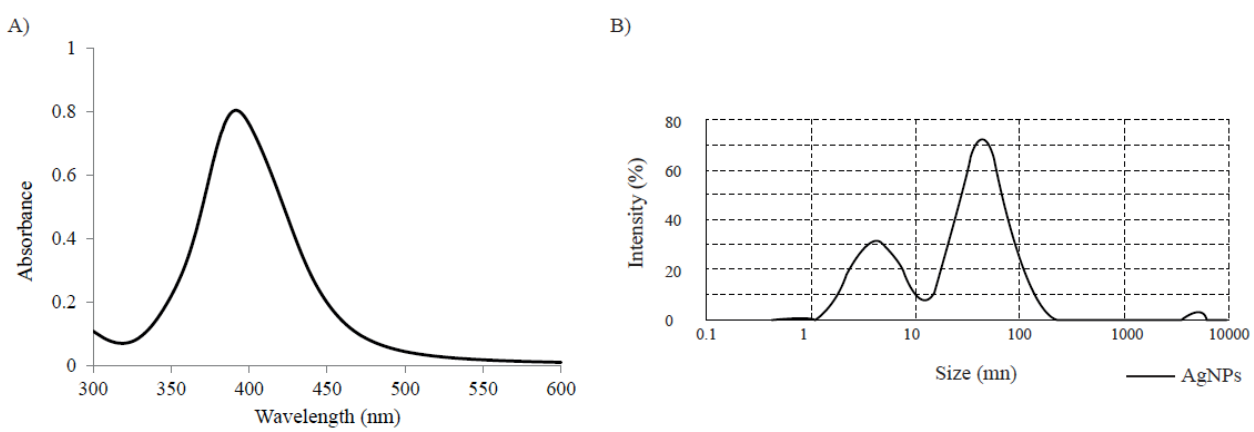

Fig. (2). (**a**) UV-Visible absorption spectra of AgNPs; (**b**) Size distribution of AgNPs by intensity.

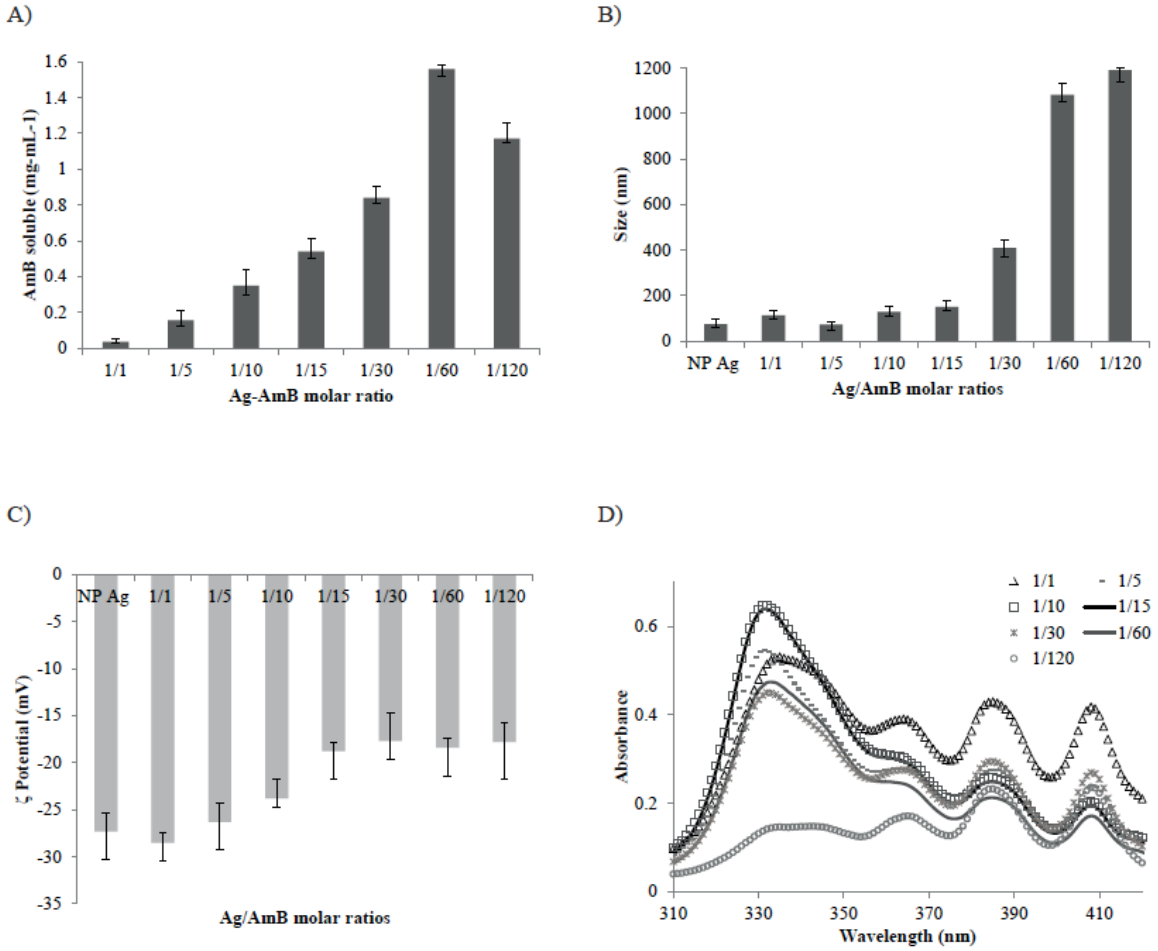

Fig. (3). (**a**) Solubilization of AmB by AgNPs at different Ag/AmB molar ratios; (**b**) Average size of AgNPs with different amounts of AmB, measured by DLS; (**c**) Average ζ potential of AgNPs with different amounts of AmB, measured by DLS; (**d**) UV-Visible absorption spectra of AgNP-AmB complexes at different Ag/AmB molar ratios. Error bars indicate the SD of the mean (n = 3).

neutral polymer and shows an uniform and ordered chain that allows it to be adsorbed easily on the surface of the particles [31]. Under these conditions more than 95 % of AmB remained soluble. The samples were translucent and concentrated to 5 mg.mL^{-1} of AmB, concentration similar to that of the commercial formulations (as Anfogen and Amfostat) of this drug (data not shown).

In parallel, we attempted to lyophilize naked AgNPs and resuspended with PEG; yet, this was not possible, demonstrating that AmB plays a fundamental role preventing the irreversible aggregation of AgNPs during the lyophilization process.

The size and ζ potential of these concentrated complexes were then measured. In Fig. (**4**) it was observed that AgNP-AmB:1/1 molar ratio seems to be the most favorable of those studied since it has a smaller and more homogeneous size (170 nm) and the most negative ζ potential (-35 mV), indicating its greater stability. In samples 1/5 and 1/10 two populations of NPs of very different size were obtained (a:70 and b:>300 nm). In these cases it is probable that the fact of having so much AmB in the cover of the AgNPs during the concentration process by lyophilization exerts the attraction and interaction between one or more particles generating larger aggregates.

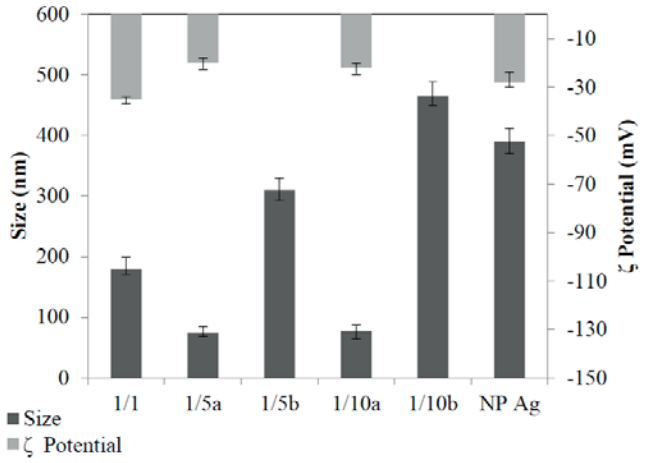

Fig. (4). Average size and ζ potential of AgNPs-AmB with 5 mg.mL^{-1} of AmB, after lyophilization and dissolution process. The indicatives of a and b for the 1/5 and 1/10 molar ratios represent the two populations observed in each case. Error bars indicate the SD of the mean (n = 3).

It is for these reasons that AgNP-AmB:1/1 molar ratio formulation was chosen to perform the studies to evaluate the cytotoxic and biological effects.

3.4. Cytotoxicity and biological activity of AgNP-AmB

The *in vitro* cytotoxic effect of AgNP-AmB was then assessed through a hemolysis assay. It was found that this formulation produces a large percentage of lysis of red blood cells, mainly because the AmB in the AgNPs associates with the cholesterol of cell membrane and breaks the cell (data not shown). However, it was shown that this lytic effect can be prevented by pre-incubating the formulation with plasma, but not with pure albumin. This indicated that there is another plasma component that binds to AmB and prevents lysis.

Some authors mention that AmB binds to cholesterol present in circulating plasma lipoproteins [32, 33]. Therefore, we wanted to evaluate whether this binding between AgNP-AmB and plasma lipoproteins is responsible for preventing hemolysis. For this purpose, the assay was repeated by pre-incubating the samples with fractions of purified LDL and HDL with a fixed cholesterol concentration (1 $mg.mL^{-1}$).

It was shown in Fig. (**5a**) that AgNP-AmB pre-incubated with plasma and purified lipoproteins are not lytic, corroborating that AmB interacts with the cholesterol in the plasma lipoproteins inhibiting their effect.

An assay was then performed to evaluate the *in vitro* cytotoxic effect of AgNP-AmB and the same samples pre-incubated with plasma on Vero and H1299 cells. Two commercial formulations were used as control, Anfogen (liposomal AmB) and Amfostat (AmB in deoxycholate micelles). Fig. (**5b**) shows that AgNPs loaded with AmB have a very strong cytotoxic effect on Vero cells. A similar effect was also observed for the formulation of AmB in micelles of deoxycholate but not for liposomal AmB. However, pre-incubation with plasma and the binding of AmB to lipoproteins inhibits this toxic effect. Similar results were obtained on H1299 cells (Fig. **5c**). Bare AgNPs do not have a cytotoxic effect on Vero nor H1299 cells (data not shown).

The antifungal effect of AgNPs and AgNP-AmB against Candida albicans was then evaluated and compared with that produced by the commercial formulations Anfogen and Amfostat. It was also evaluated whether the association with plasma lipoproteins produces some change in the antifungal activity of the nanoparticle.

In this study it was shown that AgNPs do not inhibit the growth of the fungus (data not shown). On the other hand, the results of Fig. (**5d**) show that all formulations pre-incubated with plasma have a greater antifungal effect than their corresponding plasma-free controls, thus the association of AmB with plasma lipoproteins does not prevent the drug from exerting its effect but is even increasing it somehow.

An assay was also carried out to evaluate the bactericidal effect of these AgNP-AmB nanoparticles (Fig. **5e**). It was observed that naked AgNPs have a strong bactericidal effect, greatly reducing the growth of Pseudomona aeruginosa (gram negative bacteria model). AgNPs-AmB proved to maintain the bactericidal effect of silver, being slightly more effective in preventing bacterial growth than bare NPs. However, a particularly interesting finding was observed with the AgNP-AmB sample pre-incubated with plasma. In this case a decrease was observed in the bactericidal effect of the formulation. This was probably because the coating of the nanostructure with plasma lipoproteins partially blocks the effect of silver preventing the binding of the nanoparticle to microbes.

This result is contrary to that observed for antimycotic effect of the nanostructure against Candida albicans, where pre-incubation with plasma does not prevent this effect but even increases it. This can be explained by the fact that AmB has more affinity for the ergosterol of the wall of the fungi than for the cholesterol of the plasma lipoproteins. Therefore, in the presence of both, AgNP-AmB-Lipoprotein complex inclines to the ergosterol, releases the lipoproteins and exerts its antifungal effect.

4. DISCUSSION

In this work, a simple and low-cost method has been used to synthesize AgNPs functionalized with AmB.

The stability of nanomaterials is a very important quality that must be evaluated before exploring their biomedical applications. PEG 4000 was selected as the molecule which produces the greatest stabilization of the complex. PEG proved to be the only molecule, within a battery of molecules evaluated, capable of dissolving AgNP-AmB after the lyophilization process, achieving stable complexes with invariable spectral characteristics for at least one month (data not shown). However, PEG was not able to dissolve naked AgNPs after lyophilization. This result clearly demonstrates that the association of AmB plays a fundamental role in stabilizing AgNPs, preventing the irreversible agglomeration of the nanostructures during the lyophilization process.

The colloidal stability of AgNP-AmB was also evaluated by determination of the ζ potential, which indicates the degree of repulsion between adjacent particles similarly charged in the dispersion medium. In general it is considered that the farther the value of ζ is from zero, the more stable is the particle [34, 35]. In our case, we generated fairly stable AgNP-AmB with negative ζ potential values around -30 mV.

Another factor that demonstrated the great stability of these new nanoparticles is related to the fact that during their preparation it was not observed that any material precipitated after the centrifugation of the sample for 10 min at 15,000 *xg* nor that they were disarmed by the dialysis process (see materials and methods section 2.2.2). However, it was demonstrated by in-vitro studies that the binding of AmB and AgNPs is not irreversible since this nanostructure maintains the antifungal effect of AmB as much as the bactericidal effect of silver. This means that just when the nanostructure comes into contact with a cell membrane (whether of fungi or bacteria), the active substances are released to perform their function.

With respect to the hydrodynamic radius of these NPs, it was observed that during the synthesis of the bare AgNPs, two populations were generated, the majority with a size of 50 nm while the minority a size of 5 nm. The interaction of AgNPs with AmB generated structures of increasing size according to the amount of drug added, reaching sizes of up to 1200 nm in the Ag/AmB:1/120 molar ratio. The minority population of 5 nm was only observed in the Ag/AmB:1/1 molar ratio, where the aggregated AmB content is low. From

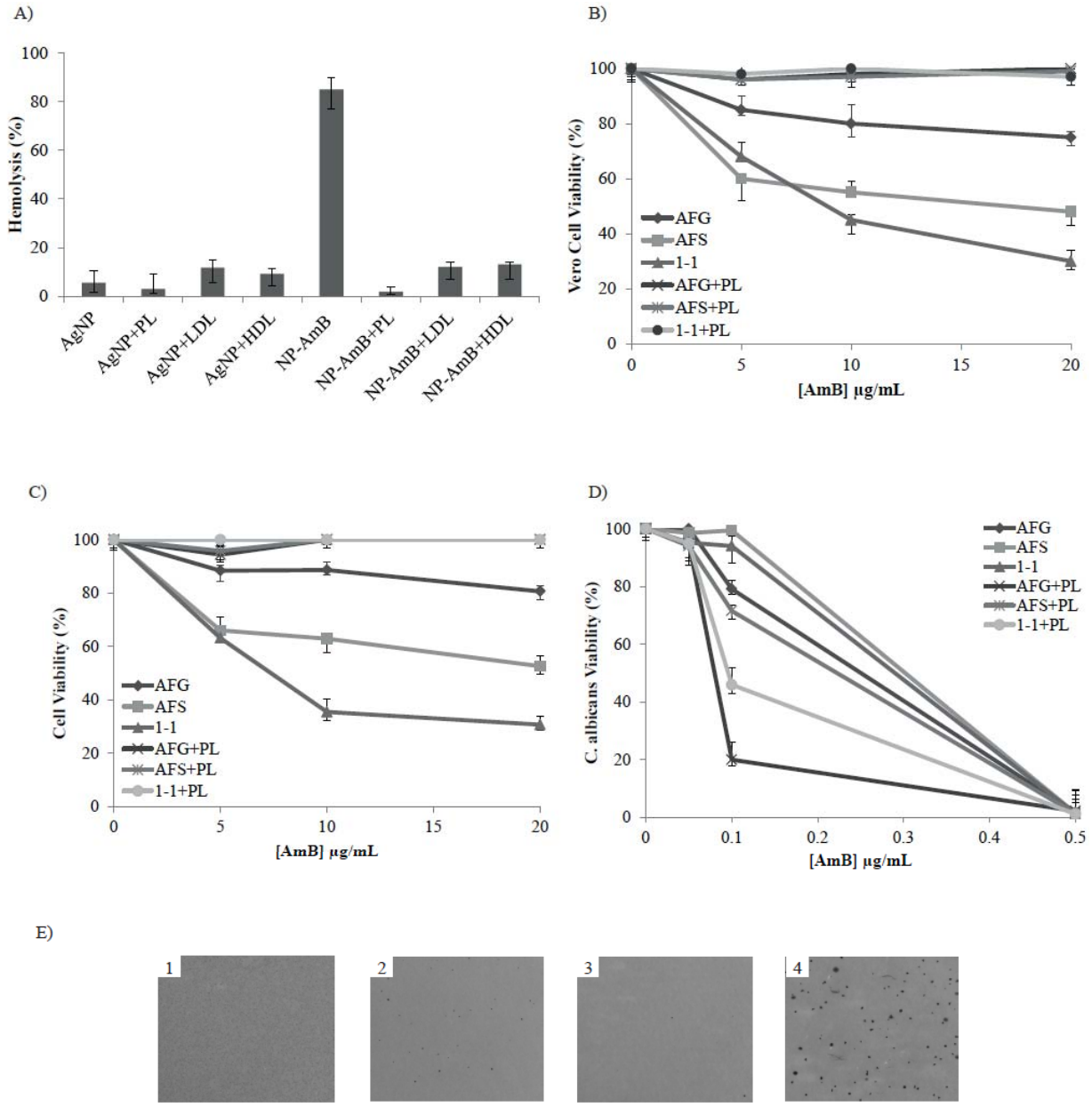

Fig. (5). *In vitro* Assays. (**a**) Hemolytic effect of AgNP and AgNP-AmB alone or with a pre-incubation with plasma (PL), low-density lipoproteins (LDL) and high-density lipoproteins (HDL); (**b**) Cytotoxic effects produced by the different formulations with or without pre-incubation with plasma (PL) on Vero cells; (**c**) Cytotoxic effects produced by the different formulations with or without pre-incubation with plasma (PL) on H1299 cells; (**d**) Biological activity of AmB produced by the different formulations with or without pre-incubation with plasma (PL) against *Candida albicans*; (**e**) Bactericidal effect of: 1- *P. aeruginosa* control; 2- AgNP; 3- AgNP-AmB:1/1; 4- AgNP-AmB:1/1+PL.
Error bars indicate the SD of the mean (n = 3).

this instance and to the extent that more AmB was added, this population disappeared.

Considering that the length of an AmB molecule is 2.4 nm [36], it can be deduced that not only a layer of AmB binds to the surface of the NP, but that multiple layers of AmB surrounding the metal structure are formed. This is possible due to the amphoteric nature of AmB and its ability to self-aggregate in aqueous solution to remain soluble [37, 38]. This feature is reflected in the absorption spectra of AgNP-AmB, where it is observed that as the AmB ratio increases, the drug is in an aggregated state with the characteristic absorption peak of this state at 333 nm. This self-aggregation capability of AmB gives the nanostructure a loading capacity far superior to that of other commercial AmB formulations. For example, Fungizone (and its analogue Amfostat used in this work) uses 4 mg of deoxycholate to generate micelles and solubilize 5 mg of AmB while AmBisome (and its analogue Amphogen used in this work) uses about 35 mg of lipids to generate liposomes and solubilize 5 mg of AmB [39, 40]. In our formulation of AgNP-AmB with an Ag/AmB:1/1 molar ratio, which proved to be the most appropriate for generating uniform-sized structures, 0.8 mg

of Ag was used to solubilize 5 mg of AmB. Moreover, the maximum loading capacity of these NPs was evidenced in the ratio Ag/AmB:1/60 where only 0.02 mg of Ag is required to solubilize 5 mg of AmB, ie AgNP loads around 250 times its own mass in AmB.

In previous studies we have shown that micelles formed by ganglioside GM1 are capable of being an appropriate carrier for AmB [41]. In this case more than 40 mg of GM1 is required to generate micelles and solubilize 5 mg of AmB. Hence our results demonstrate that AgNPs proved to be the structure with greater loading capacity of this potent antifungal drug.

It has been known for many years that silver colloids have antimicrobial properties; indeed, they have been used extensively for the treatment of burns [42, 43]. Since it is possible that the modification of the surface of these nanoparticles with certain ligands or polymers can alter their antimicrobial activity [43], it is important to carry out an evaluation. In our case it was shown that AgNP-AmB, despite being functionalized with a drug (AmB) and a polymer (PEG) on its surface maintain the bactericidal effect of silver and is even slightly superior to that obtained with naked AgNPs.

Many authors report that the bactericidal effect of AgNP depends on size [44] and that this is stronger when size is smaller due to the large surface area they have to contact with the bacterial cells [45]. However, although AgNP-AmB synthesized in this work have an average size of 170 nm, they were shown to maintain a strong bactericidal effect.

On the other hand, AgNP-AmB showed a marked toxic effect on human red blood cells and also on Vero and H1299 cell lines. This is probably due to the molecular organization of AmB in the nanostructure, since it adopts an aggregate state that allows the association of large amounts of drug with AgNP surface and this state has been described as quite more toxic than that when the drug was found in monomeric form [46, 47]. However, it was shown that AgNP-AmB are able to bind to plasma lipoproteins because of the high affinity of AmB for cholesterol; in this way, the toxic effect on the different cell types tested was inhibited. In this respect it should be noted that the association of AmB of the NPs with plasma lipoprotein cholesterol was shown to be reversible since, in the presence of ergosterol in the plasma membrane of fungi, the drug has more affinity for this and can exert its antifungal effect.

There are currently several studies demonstrating the versatility of AgNPs and their potential use as carriers of one or more drugs. In one study, presented by Krzysztof Tutaja *et al*., AmB is used both as the reducing and stabilizing agent of AgNPs to achieve monodisperse populations of AgNP-AmB with 7 nm [48]. It has also recently been shown that AgNPs may have cytotoxic effects preferentially on cancer cells without attacking normal cells, thus a number of strategies have been developed for their use in the treatment of cancer. In research published by Gopakumar *et al.* AgNPs were used to transport Sanazole and Doxorubicin, reaching high levels of induction of cytotoxicity and apoptosis in cancer cells, as well as a large reduction in tumor volume and a delay in tumor growth [49].

CONCLUSION

In this work, it was possible to synthesize AgNPs associated with AmB, a potent antimycotic, with the potential of being a new nanostructure used in medical treatments.

AgNPs-AmB were characterized by UV-visible absorption spectroscopy and DLS techniques. It was demonstrated that structures of nanometric size and high stability were formed in aqueous solution given its high ζ potential value.

It is important to emphasize that the loading capacity of AmB from these AgNPs is much higher than that of the existing micellar and liposomal formulations.

Functionalization of AgNPs with AmB and its subsequent dissolution with PEG did not alter the intrinsic antibacterial activity of silver. It was also observed that AmB solubilized in the NP is accessible and is able to bind to cholesterol present in plasma lipoproteins. However, in the presence of ergosterol of the membrane of the fungi, it is able to release cholesterol and bind to ergosterol for which it has more affinity and therefore exert its antifungal effects.

This work opens the possibility of using AgNPs as a platform to transport different poorly soluble molecules.

ETHICS APPROVAL AND CONSENT TO PARTICIPATE

Not applicable.

HUMAN AND ANIMAL RIGHTS

No Animals/Humans were used for studies that are base of this research.

CONSENT FOR PUBLICATION

Not applicable.

CONFLICT OF INTEREST

The authors declare no conflict of interest, financial or otherwise.

ACKNOWLEDGEMENTS

VL, RVA and DMB are staff members of CONICET (Consejo Nacional de Investigaciones Científicas y Tecnológicas). We wish to acknowledge Carolina Mosconi for her technical assistance with English grammar and spelling.

REFERENCES

[1] Yang, X.X.; Li, C.M.; Huang, C.Z. Curcumin modified silver nanoparticles for highly efficient inhibition of respiratory syncytial virus infection. *Nanoscale*, **2016**, 8 (5), 3040–3048.

[2] Maillard, J.Y.; Hartemann, P. Silver as an antimicrobial: facts and gaps in knowledge. *Crit. Rev. Microbiol.*, **2013**, 39, 373–383.

[3] Zhang, L.; Chen, L.; Chen, L.W.; Zhu, G. A facile synthesis of flower-shaped TiO_2/Ag microspheres and their application in photocatalysts. *RSC. Adv*., **2014**, 4, 54463–54468.

[4] Markowska, K.; Grudniak, A.M.; Wolska, K.I. Silver nanoparticles as an alternative strategy against bacterial biofilms. *Acta Biochim. Pol.*, **2013**, 60, 523–530.

[5] Zhang L. Self-assembly Ag nanoparticle monolayer film as SERS Substrate for pesticide detection. *Appl. Surf. Sci.*, **2013**, 270, 292–294.

[6] Mahajan, S.D.; Aalinkeel, R.; Law, W.C.; Reynolds, J.L.; Nair, B.B.; Sykes, D.E.; Yong, K.T.; Roy, I.; Prasad, P.N.; Schwartz, S.A. Anti-HIV-1 nanotherapeutics: promises and challenges for the future. *Int. J. Nanomedicine*, **2012**, 7, 5301-5314.

[7] Lewis, L.N. Chemical catalysis by colloids and clusters. *Chem. Rev*., **1993**, 93, 2693-2730.

[8] Bönnemann, H.; Richards, R.M. Nanoscopic Metal Particles − Synthetic Methods and Potential Applications. *Eur. J. Inorg. Chem*., **2001**, 10, 2455-2480.

[9] Tolaymat, T.M.; El Badawy, A.M.; Genaidy, A.; Scheckel, K.G.; Luxton, T.P.; Suidan, M. An evidence-based environmental perspective of manufactured silver nanoparticle in syntheses and applications: a systematic review and critical appraisal of peer-reviewed scientific papers. *Sci. Total Environ*., **2010**, 408 (5), 999-1006.

[10] Alvarez-Puebla, R.A.; Aroca, R.F. Synthesis of silver nanoparticles with controllable surface charge and their application to surface-enhanced Raman scattering. *Anal Chem.*, **2009**, 81, 2280-2285.

[11] Power, A.C.; Betts, A.J.; Cassidy, J.F. Non aggregated colloidal silver nanoparticles for surface enhanced resonance Raman spectroscopy. *Analyst*, **2011**, 136, 2794-2801.

[12] Wiley, B.; Sun, Y.; Mayers, B.; Xia. Y. Shape-controlled synthesis of metal nanostructures: the case of silver. *A Eur. J.*, **2005**, *11*, 454-463.

[13] Turkevich, J.; Kim, G. Palladium: preparation and catalytic properties of particles of uniform size. *Science*, **1970**, 169(3948), 873-879.

[14] He, Y.; Du, Z.; Ma, S.; Cheng, S.; Jiang, S.; Liu, Y.; Li, D.; Huang, H.; Zhang, K.; Zheng, X. Biosynthesis, antibacterial activity and anticancer effects against prostate cancer (PC-3) cells of silver nanoparticles using Dimocarpuslonganlour. peel extract. *Nanoscale Res. lett*., **2016**, 11(1), 300.

[15] Jeong, J.K. *et al*. Hypoxia-mediated autophagic flux inhibits silver nanoparticle-triggered apoptosis in human lung cancer cells. *Sci. Rep*., **2016**, 6, 1–13.

[16] Radziuk, D.; Skirtach, A.; Sukhorukov, G.; Shchukin, D.; Möhwald H. Stabilization of silver nanoparticles by polyelectrolytes and poly(ethylene glycol). *Macromol. Rapid. Commun*., **2007**, 28, 848–855.

[17] Chappell, M.A.; Miller, L.F.; George, A.J.; Pettway, B.A.; Price, C.L.; Porter, B.E.; Bednar, A.J.; Seiter, J.M.; Kennedy, A.J.; Steevens, J.A. Simultaneous dispersion–dissolution behavior of concentrated silver nanoparticle suspensions in the presence of model organic solutes. *Chemosphere*, **2011**, 84, 1108–1116.

[18] Yang, X.; Gondikas, A.P.; Marinakos, S.M.; Auffan, M.; Liu, J.; Hsu-Kim, H.; Meyer, J.N. Mechanism of silver nanoparticle toxicity is dependent on dissolved silver and surface coating in caenorhabditiselegans. *Environ. Sci. Technol*., **2012**, 46, 1119–1127.

[19] Austin, L.A.; Kang, B.; Yen, C.W.; El-Sayed, M.A. Nuclear targeted silver nanospheres perturb the cancer cell cycle differently than those of nanogold. *Bioconjugate Chem* , **2011**, 22, 2324–2331.

[20] Suresh, A.K.; Pelletier, D.; Wang, W.; Morrell-Falvey, J.L.; Gu, B.; Doktycz, M.J. Cytotoxicity induced by engineered silver nanocrystallites is dependent on surface coatings and cell types. *Langmuir*, **2012**, 28, 2727–2735.

[21] Sing, S.; Pate, L.P.; Jaiswal, S.; Prabhune, A.A.; Ramana, C.V.; Prasad, B.L.V. A direct method for the preparation of glycolipid–metal nanoparticle conjugates: sophorolipids as reducing and capping agents for the synthesis of water re-dispersible silver nanoparticles and their antibacterial activity. *New. J. Chem.*, **2009**, 33 (3), 646-652.

[22] Bae, E.; Park, H.J.; Lee, J.; Kim, Y.; Yoon, J.; Park, K.; Choi, K.; Yi, J. Bacteria cytotoxicity of the silver nanoparticle related to physicochemical metrics and agglomeration properties. *Environ. Toxicol. Chem*., **2010**, 29 (10), 2154–2160.

[23] Baginski, M.; Cybulska, B.; Gruszecki, W.I. Interaction of polyene macrolide antibiotics with lipid model membranes. In: Liu AL, editor. *Advances in Planar Lipid Bilayers and Liposomes. Academic Press*, **2006**, 441, 269-329.

[24] Hing, A.W.; Schaefer, J.; Kobayashi, G.S. Deuterium NMR of amphotericin B derivative in mechanically aligned lipid bilayers. *Biochim. Biophys. Acta*, **2000**, 1463, 323-332.

[25] Anya, M.H. Supramolecular lipid drug delivery systems: from laboratory to clinic: a review of the recently introduced commercial liposomal and lipid based formulations of amphotericin B. *Adv. Drug Deliv. Rev*., **1997**, 24, 345-363.

[26] Ian, M.H.; Grant, P. Lipid-based amphotericin B: a review of the last 10 years of use. *Int. J. Antimicrob. Agents*, **2001**, 17, 161-169.

[27] Gaboriau, F.; Chéron, M.; Petit, C.; Bolard, J. Heat-induced super-aggregation of amphotericin B reduces its *in vitro* toxicity: a new way to improve its therapeutic index. *Antimicrob. Agents and Chem*., **1997**, 41, 2345-2351.

[28] Wayne, P. Reference method for broth dilution antifungal susceptibility testing of yeasts. Approved standard M27-A. *National Committee for Clinical Laboratory Standards*, **1997**.

[29] Wang, A.L.; Yin, H.B.; Ren, M.; Cheng, X.N.; Zhou, Q.F.; Zhang, X.F. Effects of different functional group-containing organics on morphology-controlled synthesis of silver nanoparticles at room temperature. *Acta Metall. Sin. Engl.*, **2006**, 19, 362-370.

[30] Popa, M.; Pradell, T.; Crespo, D.; Alderón-Moreno, J.M. Stable silver colloidal dispersions using short chain polyethylene glycol. *Colloid Surf. A*, **2007**, 303 (3), 184-190.

[31] Yua, D.; Sunb, X.; Bian, J.; Tonga, Z.; Qiana, Y. Gamma-radiation synthesis, characterization and nonlinear optical properties of highly stable colloidal silver nanoparticles in suspensions. *Physica E Low Dimens. Syst. Nanostruct*., **2004**, 23, 50-55.

[32] Brajtburg, J.; Elberg, S.; Bolard, J.; Kobayashi, G.S.; Levy, R.; Ostlund, R.E.; Schlessinger, D.; Medoff, G. Interaction of plasma proteins and lipoproteins with amphotericin B. *J. Infect. Dis*., **1984**, 149, 986–997.

[33] Wasan, K.M.; Morton, R.E.; Rosenblum, M.G.; Lopez-Berestein, G. Decreased toxicity of liposomal amphotericin B due to association of amphotericin B with high-density lipoproteins: role of lipid transfer protein. *J. Pharm. Sci.*, **1994**, 83, 1006–1010.

[34] Zhang, Y.; Yang, M.; Portney, N.G. ; Cui, D.; Budak, G.; Ozbay, E.; Ozkan, M.; Ozkan, C.S. Zeta Potential: A Surface Electrical Characteristic to Probe the Interaction of Nanoparticles with Normal and Cancer Human Breast Epithelial Cells. *Biomed. Microdevices*, **2008**, 10, 321-328.

[35] Akman, E.; Genc Oztoprak, B.; Gunes, M.; Kacar, E.; Demir, A. Effect of Femtosecond Ti:Sapphire Laser Wavelengths on Plasmonic Behaviour and Size Evolution of Silver Nanoparticles. *Photon. Nanostruct.: Fundam. Appl.*, **2011**, 9, 276–286.

[36] Jarzembska, K.N.; Kamiński, D.; Hoser, A.A.; Malińska, M.; Senczyna, B.; Woźniak, K.; Gagoś, M. Controlled crystallization, structure, and molecular properties of iodoacetylamphotericin B. *Cryst. Growth. Des*., **2012**, 12, 2336-2345.

[37] Legrand, P.; Romero, E.A.; Cohen, B.E.; Bolard, J. Effects of aggregation and solvent on the toxicity of amphotericin B to human erythrocytes. *Antimicrob. Agents Chemother*., **1992**, 36, 2518-2522.

[38] Wasko, P.; Luchowski, R.; Tutaj, K.; Grudzinski, W.; Adamkiewicz, P.; Gruszecki, W.I. Toward understanding of toxic side effects of a polyene antibiotic amphotericin B: fluorescence spectroscopy reveals widespread formation of the specific supramolecular structures of the drug. *Mol. Pharm.*, **2012**, 9, 1511-1520.

[39] Hamill, R. J. Amphotericin B Formulations: A Comparative Review of Efficacy and Toxicity. *Drugs*, **2013**, 73, 919–934.

[40] Adler-Moore, J- P.; Proffitt, R. T. Development, characterization, efficacy and mode of action of Ambisome, a unilamellar liposomal formulation of amphotericin B. *Journal of liposome research*, **1993**, 3, 3, 429-450.

[41] Leonhard, V.; Alasino, R.V.; Bianco, I.D.; Garro, A.G.; Heredia, V.; Beltramo, D.M. Biochemical characterization of GM1 micelles amphotericin B interaction. *Curr. Drug Deliv*., **2015**, 12 (4), 406-414.

[42] Gladitz, M.; Reinemann, S.; Radusch, H-J. Preparation of Silver Nanoparticle Dispersions via a Dendritic-Polymer Template Approach and their Use for Antibacterial Surface Treatment. *Macromol. Mater. Eng*., **2009**, 294 (3), 178-189.

[43] Melaiye, A.; Sun, Z.; Hindi, K.; Milsted, A.; Ely, D.; Reneker, D.H.; Tessier, C.A.; Youngs, W.J. Silver(I)−imidazole cyclophanegem-diol complexes encapsulated by electrospuntecophilic nanofibers: Formation of nanosilver particles and antimicrobial activity. *J. Am. Chem. Soc*., **2005**, 127, 2285-2291.

[44] Raimondi, F.; Scherer, G.G.; Kotz, R.; Wokaun, A. Nanoparticles in energy technology: examples from electrochemistry and catalysis. *Angew. Chem. Int. Ed. Engl.*, **2005**, 44, 2190–2209.

[45] Morones, J.R.; Elechiguerra, J.L.; Camacho, A.; Ramirez, J.T. The bactericidal effect of silver nanoparticles. *Nanotechnology*, **2005**, 16, 2346–2353.

[46] Legrand, P.; Romero, E.; Devissaguet, J-P.; Cohen, E.; Bolard, J.B. Effects of aggregation and solvent on the toxicity of amphotericin B to human erythrocytes. *Antimicrob. Chemical Agents*, **1992**, 36 (11), 2518–2522. [is repeated see ref 28]

[47] Torrado, J.J.; Espada, R.; Ballesteros, M.P.; Torrado-Santiago, SJ..Amphotericin B formulations and drug targeting. *J. Pharm. Sci.*, **2008**, 97 (7), 2405-2425.

[48] Tutaj, K.; Szlazak, R.; Szalapata, K.; Starzyk, J.; Luchowski, R.; Grudzinski, W.; Osinska-Jaroszuk, M.; Jarosz-Wilkolazka, A.; Szuster-Ciesielska, A.; Gruszecki, W.I. Amphotericin B-Silver Hybrid Nanoparticles: Synthesis, Properties and Antifungal Activity. *Nanomedicine: NBM*, **2016**,12 (4), 1095-1103.

[49] Nair, G.G.; Nair, C.K.K. Sanazole (AK) and DOX were complexed with SNPs, individually and in combination to obtain SN-AK, SN-DOX, and SN-AK-DOX. *J. Can. Res. Ther.*, **2014**, 10 (4), 979-984.